L-3,3',5-triiodothyronine and pregnenolone sulfate inhibit *Torpedo* nicotinic acetylcholine receptors

Steven X. Moffett[1], Eric A. Klein[1,2], Grace Brannigan[1,3], Joseph V. Martin[1,2]*

1 Center for Computational and Integrative Biology, Rutgers University—Camden, Camden, New Jersey, United States of America, **2** Department of Biology, Rutgers University—Camden, Camden, New Jersey, United States of America, **3** Department of Physics, Rutgers University—Camden, Camden, New Jersey, United States of America

* joe.martin@rutgers.edu

Abstract

The nicotinic acetylcholine receptor (nAChR) is an excitatory pentameric ligand-gated ion channel (pLGIC), homologous to the inhibitory γ-aminobutyric acid (GABA) type A receptor targeted by pharmaceuticals and endogenous sedatives. Activation of the $GABA_A$ receptor by the neurosteroid allopregnanolone can be inhibited competitively by thyroid hormone (L-3,3',5-triiodothyronine, or T3), but modulation of nAChR by T3 or neurosteroids has not been investigated. Here we show that allopregnanolone inhibits the nAChR from *Torpedo californica* at micromolar concentrations, as do T3 and the anionic neurosteroid pregnenolone sulfate (PS). We test for the role of protein and ligand charge in mediated receptor inhibition by varying pH in a narrow range around physiological pH. We find that both T3 and PS become less potent with increasing pH, with remarkably similar trends in IC_{50} when T3 is neutral at pH < 7.3. After deprotonation of T3 (but no additional deprotonation of PS) at pH 7.3, T3 loses potency more slowly with increasing pH than PS. We interpret this result as indicating the negative charge is not required for inhibition but does increase activity. Finally, we show that both T3 and PS affect nAChR channel desensitization, which may implicate a binding site homologous to one that was recently indicated for accelerated desensitization of the $GABA_A$ receptor by PS.

Introduction

The nicotinic acetylcholine receptor (nAChR) is an excitatory receptor protein localized in the central nervous system [1], the peripheral nervous system and neuromuscular junction (reviewed in [2]). Pathologies of the receptor, including epilepsy [3] and myasthenia gravis (in muscle-type nAChRs) [4, 5], demonstrate its crucial function in fast synaptic transmission. In muscle-type nAChRs, it is a cation-conducting member of the pentameric ligand-gated ion channel (pLGIC), or "Cys-loop" receptor superfamily [6–10]. Of the five homologous subunits that comprise the nAChR structure and central pore, two are identical (α, γ, α, β, δ). When acetylcholine molecules bind to the α-γ and α-δ subunit interfaces in the receptor's extracellular

domain (ECD), conformational changes propagate to its transmembrane domain (TMD). Four alpha helices (M1-M4) from each subunit form the TMD, with the M2 helices from each subunit lining the receptor's central pore. Upon binding acetylcholine, the central pore's inner diameter increases, permitting ion flux through the channel [11].

The pLGIC superfamily also includes glycine receptors, 5-HT$_3$ receptors, and γ-aminobutyric acid (GABA$_A$) receptors [6], as well as a range of homologs in invertebrates, plants, and prokaryotes [12]. Neurosteroids, either those synthesized in endocrine glands and metabolized, or those synthesized *de novo* in brain tissue, can have hypnotic [13], anxiolytic [14], anxiogenic [15], anti-convulsant [16], and analgesic effects (for review see [17]), and can have synergistic effects with anesthetics [18, 19]. Previous investigations of pLGICs elucidated structure-function relationships of neurosteroids' molecular features [20–23]. The distinction between molecular features of otherwise similar compounds provides insight into binding sites on the receptor; closely-related molecular species can have differing [22, 24] or opposing [10, 25] effects on their target receptor, and the same neurosteroid can have differing effects on alternative receptor isoforms [26–28].

The neurosteroid 3α-hydroxy-5α-pregnan-20-one (allopregnanolone) activates the GABA$_A$ receptor [29], as does the related 5α-pregnane-3α,21-diol-20-one (THDOC) [30–32]. The thyroid hormone L-3,3',5-L-triiodothyronine (T3) (Fig 1A) was originally theorized to have neurosteroid-like effects due to its similarity to neurosteroids' size, shape, and lipophilicity [33]. In particular, the results of computational analysis of the overall volumes and shapes of pregnanolone sulfate (PS) and T3 are compared in Figs 5 and 6 of our previous study [33}. Superpositioning of the two molecules showed that not only the molecular volumes, but also the shapes, are nearly identical, and no unmatched functional groups extend from the main axis. Additionally, we have previously published molecular dynamics simulations of single molecules of T3 and allopregnanolone (see S1 Movie and S2 Movie of [29]), illustrating the rigidity of these two molecules in an aqueous solution. The rigidity of the steroid scaffold can be compared to the rigidity of T3 due to the steric hindrance due to the two iodines on the inner aromatic ring of T3."

Despite structural analogy to positive allosteric modulators, T3 inhibits activity of the GABA$_A$ receptor at low concentrations [29, 34–36] and competitively inhibits GABA$_A$ receptor activation due to ivermectin or allopregnanolone [29]. The mechanism underlying this surprising result is unknown, and here we test the hypothesis that a population of anionic T3 at physiological pH interacts with pLGICs through a similar mechanism as the anionic neurosteroid pregnanolone sulfate (PS) (Fig 1B). PS is sulfated at C3 but is otherwise similar to positively-modulating neurosteroids, and also inhibits GABA$_A$ receptor function [37].

Structural biology has recently provided insight into the binding mode of PS with GABA$_A$ receptors. In a recent crystal structure of a homopentameric receptor chimera comprised of a *Gleobacter* ligand-gated ion channel (GLIC) ECD and a mouse GABA$_A$R α$_1$ TMD, Laverty et al. [38] showed that PS binds alongside a groove between the M3 and M4 helices near the intracellular side of the transmembrane domain of GABA$_A$ receptors. This site is involved with the "desensitization gate" recently classified by Gielen et al. [39], indicated by mutations of amino acid residues at the M1-M2 linker and M3 helix of GABA$_A$ receptors affected receptor desensitization.

While lipid mixtures used for X-ray crystallography of membrane proteins have become more complex, there are still significant discrepancies with native membranes. pLGICs are extremely lipid sensitive; in particular, they may have specific interactions with anionic lipids [40, 41], polyunsaturated fatty acids [42], and cholesterol [43, 44]. The most feasible pLGIC for study in native membranes is the nicotinic acetylcholine receptor, due to its high concentration in the electric organ of the torpedo electric ray.
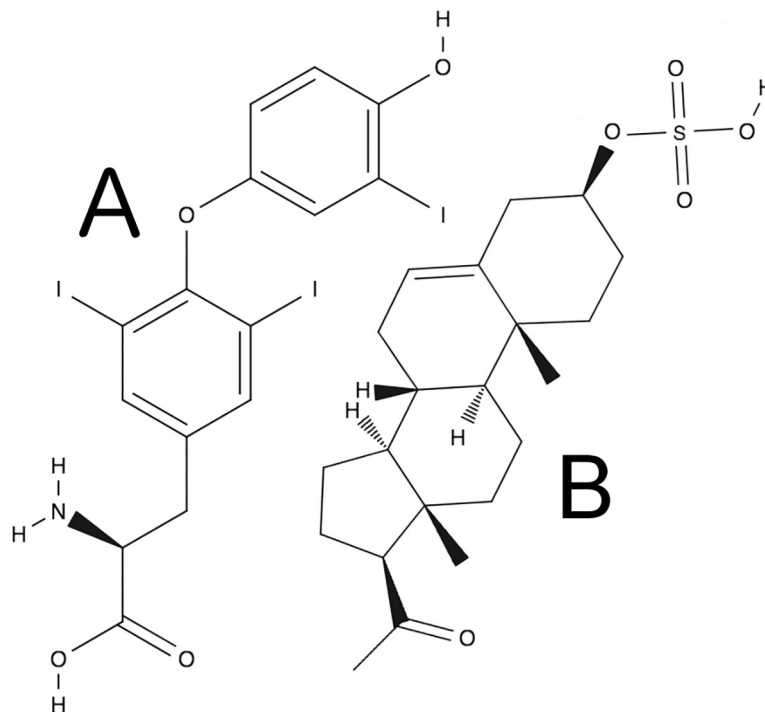
Fig 1. Molecular structure of T3 and PS. Comparisons of structures of the thyroid hormone T3 (A) and the neurosteroid PS (B). T3 and neurosteroids share common features including molecular volume and size, placement of hydrogen-bond accepting groups, presence of carboxylic residues projecting from rings, and charged headgroups.

https://doi.org/10.1371/journal.pone.0223272.g001

Lipophilic modulators often have opposite effects on nAChRs and GABA$_A$ receptors; for example, nonhalogenated and halogenated alkane anesthetics inhibit nAChRs but potentiate GABA$_A$ receptors (for review see [45]). Most known neurosteroids inhibit nAChRs, regardless of their effect on GABA$_A$Rs. Progesterone, dehydroepiandrosterone sulfate (DHEAS), hydrocortisone, and 3α,5α,17β-3-hydroxyandrostane-17-carbonitrile (ACN) inhibit rat neuronal nAChRs [23, 24], while progesterone, estradiol, corticosterone, and dexamethasone non-competitively inhibit human muscle-type [46, 47], ganglionic [46], and *Torpedo* nAChRs [48]. Several lipophilic molecules, including anesthetics and cholesterol, affect both GABA$_A$Rs and nAChRs [49–52]. While PS inhibits nAChR-regulated release of catecholamines from the adrenal medulla [53], no effect of PS on nAChR binding was previously seen. Here we report, for the first time, an inhibitory influence of PS on receptor function in muscle-type nAChRs.

Changes in extracellular pH also affect nAChR ion conductance, with more acidic environments yielding lower ion flux and basic environments yielding higher ion flux relative to the receptor's acetylcholine response at a neutral pH [54, 55]. Different pH environments also affect mean open channel time and desensitization of the receptor [55]. Palma et al. [54] and Li et al. [55] showed that pH changes in the surrounding fluid correlate with changes in nAChR channel conductivity, suggesting that charged residues in the nAChR vestibular and channel pore region affect allosteric transitions to active and inactive states, and that changes in the extracellular pH would titrate these residues. Here we control for the effect of pH on receptor function by comparison of pH effects on modulation by T3 with those of PS, which is not expected to change charge states over the pH range we consider.

We tested the hypothesis that a population of anionic T3 transduces inhibition of nAChR at physiological pH. by extracting functional nAChRs from *Torpedo californica* and used two-electrode voltage clamp (TEVC) to demonstrate functional effects of PS and T3 on nAChRs.

We found that both PS and T3 inhibit nAChR activity due to acetylcholine, representing a case in which the same effect on channel function is demonstrated in both nAChRs and $GABA_A$ receptors. We also performed TEVC in differing extracellular pH environments to demonstrate the differential effects pH has on ligand charge and resultant receptor activity. Further, we show that PS and T3 modulate the effects of different pH environments on current amplitude when binding acetylcholine. We also show that T3 and PS change nAChR kinetics, increasing desensitization rate at low pHs but minimally affecting desensitization rate at high pHs.

Materials and methods

Chemicals

Carbachol, acetylcholine, dimethyl sulfoxide (DMSO), asolectin, T3, NaOH, allopregnanolone, and pregnenolone sulfate were purchased from Sigma Aldrich (St. Louis, MO). Isoflurane was purchased from Henry Schein Animal Health (Dublin, OH). T3 was dissolved in 0.1 M NaOH. Allopregnanolone was dissolved in 0.1% DMSO. All other ligands were dissolved directly in modified Barth's solution (88 mM NaCl; 1 mM KCl; 0.4 mM $CaCl_2$; 0.33 mM Ca $(NO_3)_2$; 0.8 mM $MgSO_4$; 5 mM tris(hydroxymethyl)aminomethane-HCl (Tris-HCl); 2.4 mM $NaHCO_3$); at low or high pHs, Tris-HCl was replaced with either 2-(*N*-morpholino)ethanesulfonic acid (MES) (T3/PS experiments at pH 6–6.7) or *N*-2-hydroxyethylpiperazine-*N'*-2-ethanesulfonic acid (HEPES) (T3 experiments at 8–9).

Preparation of crude *Torpedo* nicotinic acetylcholine receptors

All steps before microinjection of resuspended receptor proteins were performed at 0 to 4 ˚C and were modified from the preparation method described previously [56]. Briefly, flash-frozen *Torpedo* electric organ was purchased from Aquatic Research Consultants (San Pedro, CA). The frozen tissue (600 g) was homogenized in homogenization buffer (10 mM sodium phosphate, 5 mM ethylenediaminetetraacetic acid (EDTA), 5 mM ethylene glycol-bis(β-aminoethyl ether)-N,N,N′,N′-tetraacetic acid (EGTA), 10 mM iodoacetamide, 0.1 mM phenylmethylsulfonyl fluoride (PMSF), 0.02% NaN_3, pH 7.5) in 30-second bursts at liquefaction setting (Oster blender) and centrifuged for 10 min at 4,080 x g. The supernatant was then filtered through 4 layers of cheesecloth and reserved. The pellets were then resuspended in 200 mL homogenization buffer and centrifugation was repeated. All of the supernatants were then pooled and centrifuged at 134,000 x g for 45 minutes. This pellet was resuspended in 32 mL 28% (w/v) sucrose buffer (10 mM sodium phosphate, 0.1 mM EDTA, 0.02% NaN_3, pH 7.0). In order to isolate membrane proteins, the aliquots of resuspended pellet (8 mL each) were layered on top of a discontinuous sucrose gradient (10 mL 30% sucrose, 12 mL 35% sucrose, 7 mL 41% sucrose) and centrifuged at 121,800 x g for 4 hours. The membrane band at the interface of the 30–35% sucrose layer was collected using a thin glass transfer pipet, diluted 1:1 with deionized water, and centrifuged at 142,400 x g for 35 minutes. The membranes in the resulting pellet were base-extracted by resuspending them to approximately 0.5 mg/mL protein in water, and the pH was carefully titrated to 11.0 with NaOH, followed by stirring for 45 minutes. The base-extracted membranes were then centrifuged at 142,400 x g for 45 minutes, resuspended in buffer A (100 mM NaCl, 10 mM Tris-HCl, 0.1 mM EDTA, 0.02% NaN_3, pH 7.4), and flash-frozen in liquid nitrogen.

Solubilization of crude nicotinic acetylcholine receptor

The protein product from extraction was diluted to 2 mg protein/mL in buffer A. Sodium cholate (10% w/v) dissolved in buffer A was added to give a final cholate concentration of 1%. The

mixture was then stirred for 30 minutes, centrifuged at 142,400 x g for 30 minutes, and the supernatant was collected.

Preparation of asolectin liposomes for resuspension

Solid asolectin lipid was suspended in 4.16% cholate solution in buffer A to form a 65 mM solution. The mixture was vortexed and sonicated at 20 ˚C under argon gas for 45 minutes, and then stored at 0–4 ˚C until reconstitution.

Reconstitution of *Torpedo* nicotinic acetylcholine receptors in asolectin liposomes

Solubilized nAChRs (1–1.65 mg/mL) were mixed with 0.3 mL of liposome/cholate mixture to yield a final volume of 1 mL, and a final concentration of 2% cholate. The mixture was dialyzed for 48 hours against 1,000 volumes buffer A, with a change of buffer every 12 hours. Before use in dialysis, buffer A was bubbled with argon gas for 15 minutes.

Oocyte microinjection

Ready-to-inject, defolliculated *Xenopus* oocytes were purchased from Ecocyte Bioscience (Austin, TX). The glass injectors were 1.6 to 2 mm o.d., 1.2 to 1.6 mm i.d., and were pulled using a Sutter Instrument Co. Model P-97 puller. The oocytes were injected with 46 nL asolectin-resuspended nAChRs using a digital microdispenser (Drummond Nanoject II). The injected oocytes were incubated at 19 ˚C in sterile Standard Barth's solution (SBS; 88 mM NaCl; 1 mM KCl; 0.4 mM $CaCl_2$; 0.33 mM $Ca(NO_3)_2$; 0.8 mM $MgSO_4$; 5 mM Tris-HCl; 2.4 mM $NaHCO_3$) supplemented with 50 mg/L gentamicin.

Two-electrode voltage clamping of oocytes

Sixteen hours after injection, the oocytes were clamped using a TEVC system. All ligands were dissolved in modified Barth's solution at the indicated pH and were perfused into the chamber using a gravity-flow system. Thyroid hormones were initially dissolved in 0.1 M NaOH. The oocytes were impaled with two 3 M KCl-filled glass microelectrodes (1–2 MΩ each) and were clamped at -60 mV with an OC-725C Oocyte Clamp (Warner Instruments). Acetylcholine was applied to the bath surrounding the oocyte using a gravity-flow system at 10–13 mL/min. T3 or PS were co-applied with acetylcholine, also using a gravity-flow system. Each ligand perfusion lasted 60–70 seconds; after each perfusion, the bath solution was exchanged with ligand-free buffer until the current response signal had returned to baseline for at least 120 seconds before the next application of ligand(s). Data were recorded using iWorx LabScribe v1.959.

Data analysis

The current flux signal for each administration of ligand was exported from iWorx into Matlab version 2012b. Due to significant batch-to-batch variation of ion conductance after receptor microinjection, maximal current response (peak) values for inhibition data were normalized to each oocyte's control maximal peak. For all data related to inhibitor concentration curves, the data were fit according to the conditions specified in Table 1. The equation for the fit was Y = Bottom + (Top-Bottom)/(1+10^((LogIC50-X)*HillSlope)).

The data were then trimmed to begin with the response as it reached 0.96 of the response peak (to avoid false inflection points by signal noise just after the response's maximum point), and end 35 seconds post-peak. The data were then fit to a two-degree exponential function

Table 1. Fit types for inhibition-response curves.

Inhibitor/pH	Fit Type	IC50 (µM)	Constraints
T3/PS 7, T3 7.2	log(inhibitor) vs. response	PS 0.77; T3 1.2	Top = 100, Hill Slope = 1
T3/PS 7.5, T3 7.7	log(inhibitor) vs. response	PS 4.6; T3 1.0	Top = 100, Hill Slope = 1
T3/PS 8, T3 8.2	log(inhibitor) vs. response	PS 3.5; T3 1.6	Top = 100, Hill Slope = 1
T3/PS 8.5, T3 8.7	log(inhibitor) vs. response	PS 10.5; T3 4.7	Top = 100, Hill Slope = 1
T3/PS 9, T3 9.2	log(inhibitor) vs. response	PS 2.4; T3 7.3	Top = 100, Hill Slope = 1
Allopregnanolone	log(inhibitor) vs. response—Variable slope	20	None
Triac	log(inhibitor) vs. response	109	Top = 100, Hill Slope = 1

(i.e., slow and fast response; $y = a \times e^{-\left(\frac{x}{A_1}\right)} + b \times e^{-\left(\frac{x}{A_2}\right)}$). The slower response of the two-degree exponential function was used in each calculation for analysis of the decay rate, as small irregularities in the raw signal yielded extremely high values for the fast component. For each ligand/environmental condition (n = 3, per condition), decay response and amplitude were calculated and averaged.

Results

PS and T3 inhibit nAChRs at concentrations similar to $GABA_A$ receptor $IC_{50}s$

We co-administered several neurosteroid and neurosteroid-like ligands with acetylcholine during TEVC to determine their effects on nAChR function. Fig 2A shows the inhibitory effect of T3 on nAChR stimulation by 30 µM acetylcholine, as well as a representative trace of the reduction in response due to acetylcholine when co-applied with T3 (Fig 2A, inset). The apparent maximal effect of T3 (seen at $\geq$ 100 µM) reduced the nAChR control response by 80 ± 6%, with an IC_{50} of 5.4 ± 1 µM T3. This is very similar to the IC_{50} of T3 for the $GABA_A$ receptor (8 ± 2 µM) [29].

Fig 2B shows the inhibitory effect of PS on nAChR stimulation by 30 µM acetylcholine, as well as a representative trace of the reduction in response due to acetylcholine when co-applied with PS (Fig 2B, inset). The apparent maximal effect of PS (seen at $\geq$ 100 µM) reduced the nAChR control response by 81 ± 4%, with an IC_{50} of 4.9 ± 3 µM PS. Triiodothyroacetic acid
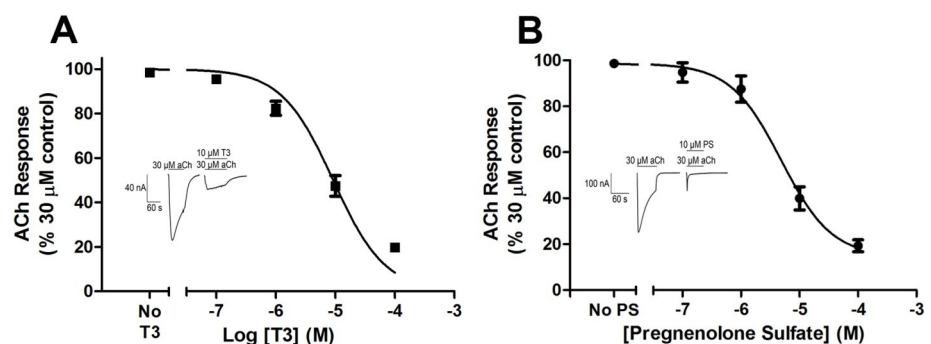
Fig 2. Inhibition of nicotinic acetylcholine receptor response to acetylcholine by T3 and PS. The inhibitory dose-response curves for T3 (A) or PS (B) on ACh-stimulated currents are represented as a percentage of the maximal, non-inhibited response to ACh. Representative tracings show current responses due to application of ACh alone and ACh with T3 (A, inset) or PS (B, inset). Horizontal lines above each trace show the onset and duration of applied ligand(s). The data are represented as mean ± standard error of the mean (SEM). For each data point, n = 3–7.
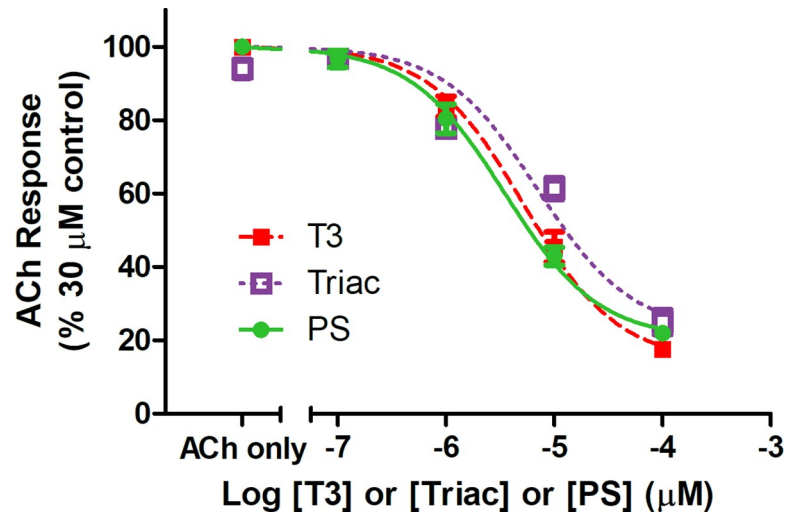
Fig 3. Inhibition of nicotinic acetylcholine receptor response to acetylcholine by T3, PS, and triac. The inhibitory dose-response curves for T3, PS, or triac on ACh-stimulated current, represented as a percentage of the maximal response to ACh. The data are represented as mean ± SEM (n = 3–7).

https://doi.org/10.1371/journal.pone.0223272.g003

(triac), which lacks the amine group of T3, also inhibits nAChR, with an IC_{50} of 7 ± 3.1 μM triac (Fig 3). Further, allopregnanolone inhibits activity of nAChRs due to carbachol, an ACh agonist (IC_{50}: 20 ± 13 μM) (Fig 4).

Both negatively-charged and neutral forms of T3 inhibit nAChR

Environmental pH affects molecular charge. According to the titration curve of T3 (Fig 5), T3's pK2 value is slightly lower than 7.3, in which the hydroxyl group becomes anionic while the amine group remains neutral. However, over this pH interval, PS is expected to retain a negative charge. At physiological pH, there are both charged PS and a proportion of charged
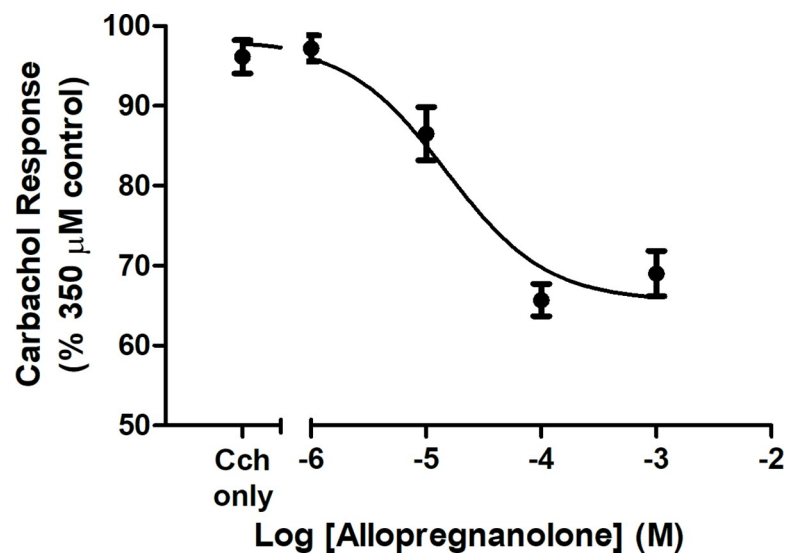
Fig 4. Inhibition of carbachol by allopregnanolone. The inhibitory dose-response curves for allopregnanolone on carbachol (Cch)-stimulated current, represented as a percentage of the maximal response to Cch. The data are represented as mean ± SEM (n = 5).

https://doi.org/10.1371/journal.pone.0223272.g004
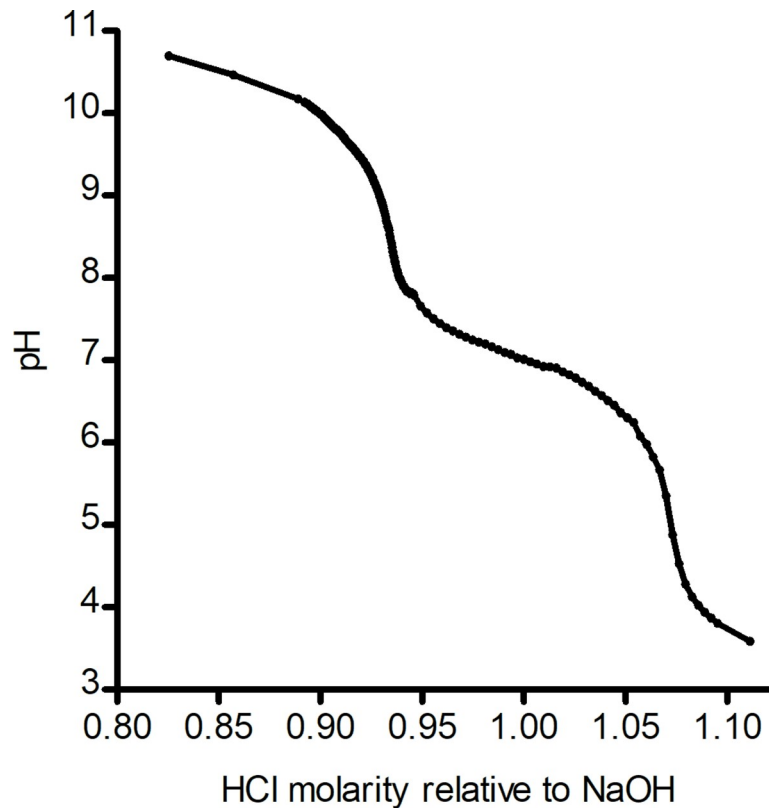
Fig 5. Titration curve of T3. The pK2 value of T3 is ~7.19, corresponding to the deprotonation of the amine group. The (theoretical) pK1 value, corresponding to the carboxylic acid group, is 0.3, while the pK3 value, corresponding to the hydroxy group, is 12.25.

https://doi.org/10.1371/journal.pone.0223272.g005

T3 molecules. We performed TEVC tests of nAChR inhibition due to T3 at different pHs; changing the surrounding pH allowed observation of effects due to T3's amino acid (head-group) in different charge states, as well as effects due to different charge states of the amino acids on the receptor, on nAChR binding. These effects could be compared to the effect due to the unchanging PS sulfate group (headgroup) charge.

The pH environment affects inhibition of nAChRs by both T3 and PS. Dose response curves show the effect of pH (6–9, in 0.5 pH increments) on the IC_{50} of T3 and PS (Fig 6A–6G). A two-way ANOVA (for hormone and dose) indicates that pH has a significant effect on nAChR flux for experiments using T3 ($p < 0.0001$, $F_{(6, 70)} = 74.25$) or PS ($p < 0.0001$, $F_{(6, 70)} = 24.02$) and that the effect due to the pH environment and due to T3 ($p < 0.0001$, $F_{(6,70)} = 11.69$) or PS ($p < 0.0001$, $F_{(6,70)} = 6.214$) dose have interactive effects on nAChR flux.

The effects of pH on inhibition of nAChRs by T3 and PS diverge at the T3 pK2 value. From pH 6–7, the IC_{50} values of T3 and PS (Fig 6H) are similar. However, above the pK2 value of T3 (~7.3), the IC_{50} values of T3 and PS are distinct, with the T3 IC_{50}s shifting downward relative to the IC_{50} values of PS. This divergence is coincident with the increase in extracellular pH above the pK2 value of T3. The PS IC_{50} value decreases below T3's at pH 9, where the net charge of T3 becomes -1, and becomes more prominent than the neutral form dominant at lower pHs.

T3 and PS affect desensitization kinetics

Figs 8 and 9 show representative traces of inhibition due to T3 and PS over 60-second administrations. Raw traces of 0–10 μM T3 or PS at pH 6 and 7.5 (Fig 8) illustrate the effect of dose on
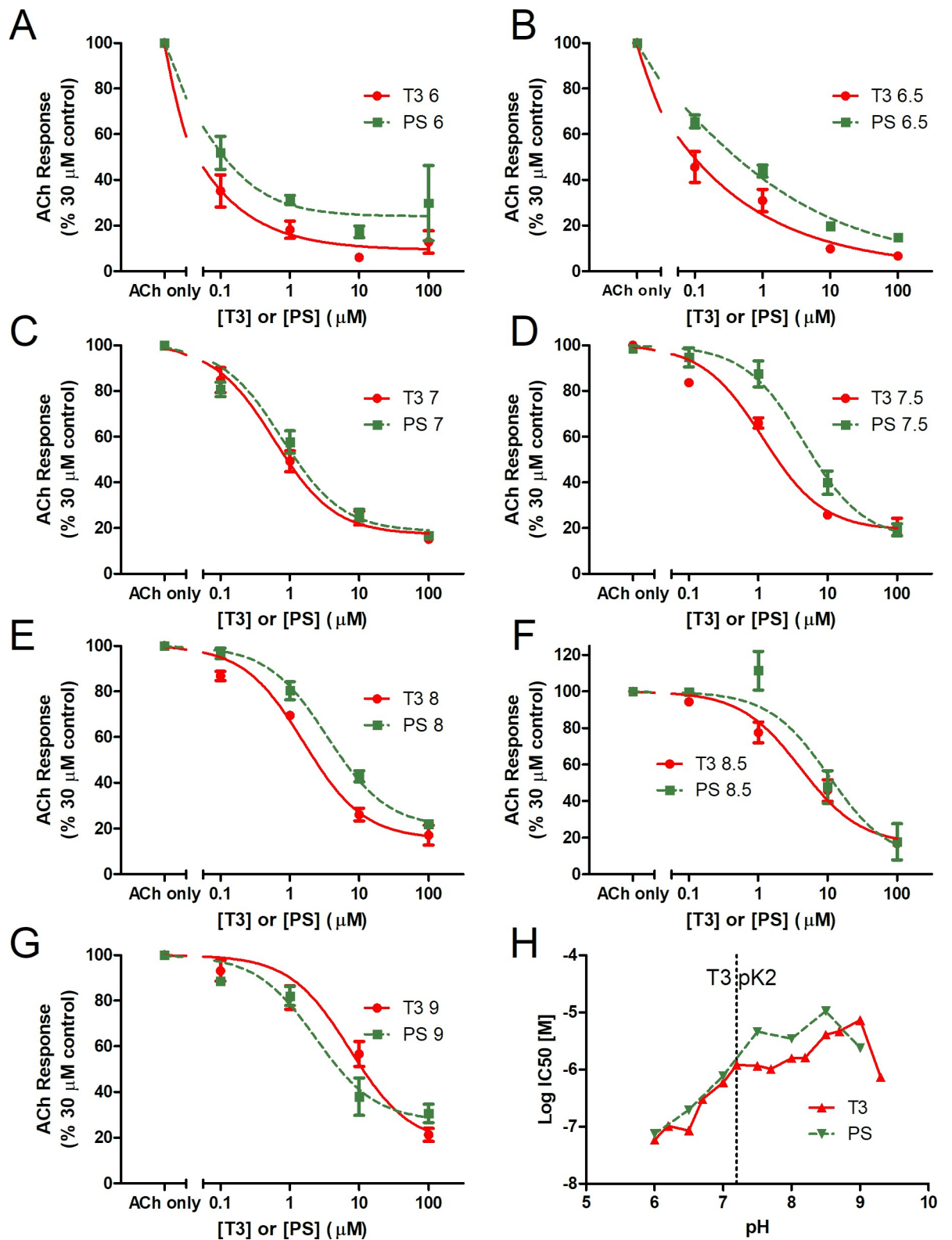
Fig 6. Effects of extracellular pH on inhibition of nAChRs by T3 and PS. The dose-response curves for T3 or PS on ACh-stimulated current were evaluated at pH (A) 6, (B) 6.5, (C) 7, (D) 7.5, (E) 8, (F) 8.5, or (G) 9. Data in (A-G) are represented as a percentage of the maximal response to ACh. The data are represented as mean ± SEM (n = 3). (H) IC_{50} values were generated from the inhibition curves at each pH interval. T3 data is supplemented with inhibition experiments run at each pH level + 0.2 (Fig 7). The dotted vertical line denotes the pK2 value of T3.
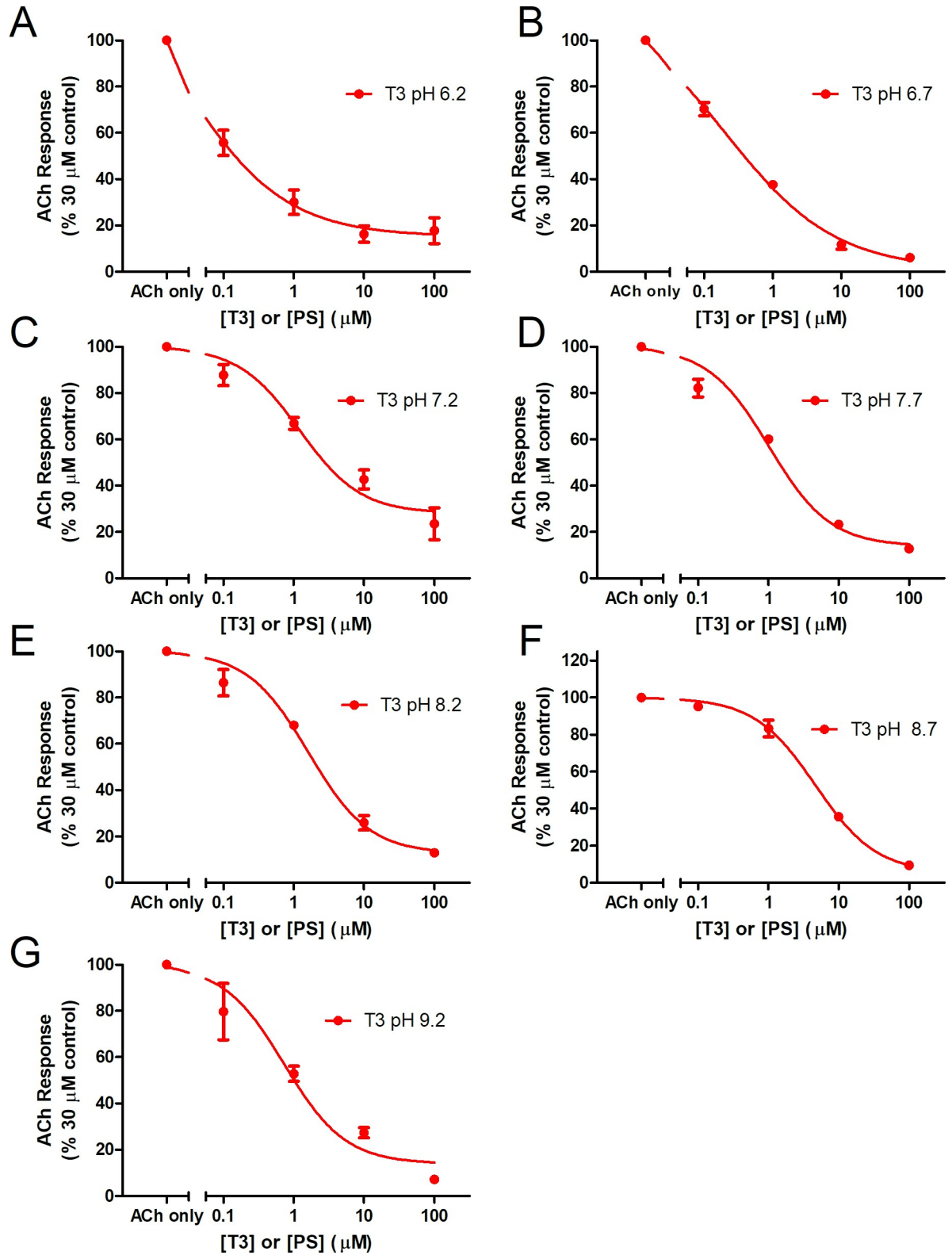
Fig 7. Effects of extracellular pH on inhibition of nAChRs by T3 at offset pHs. The dose-response curves for T3 on ACh-stimulated current were evaluated at pH (A) 6.2, (B) 6.7, (C) 7.2, (D) 7.7, (E) 8.2, (F) 8.7, or (G) 9.2. Data are represented as a percentage of the maximal response to ACh. Error bars represent ± SEM (n = 3).
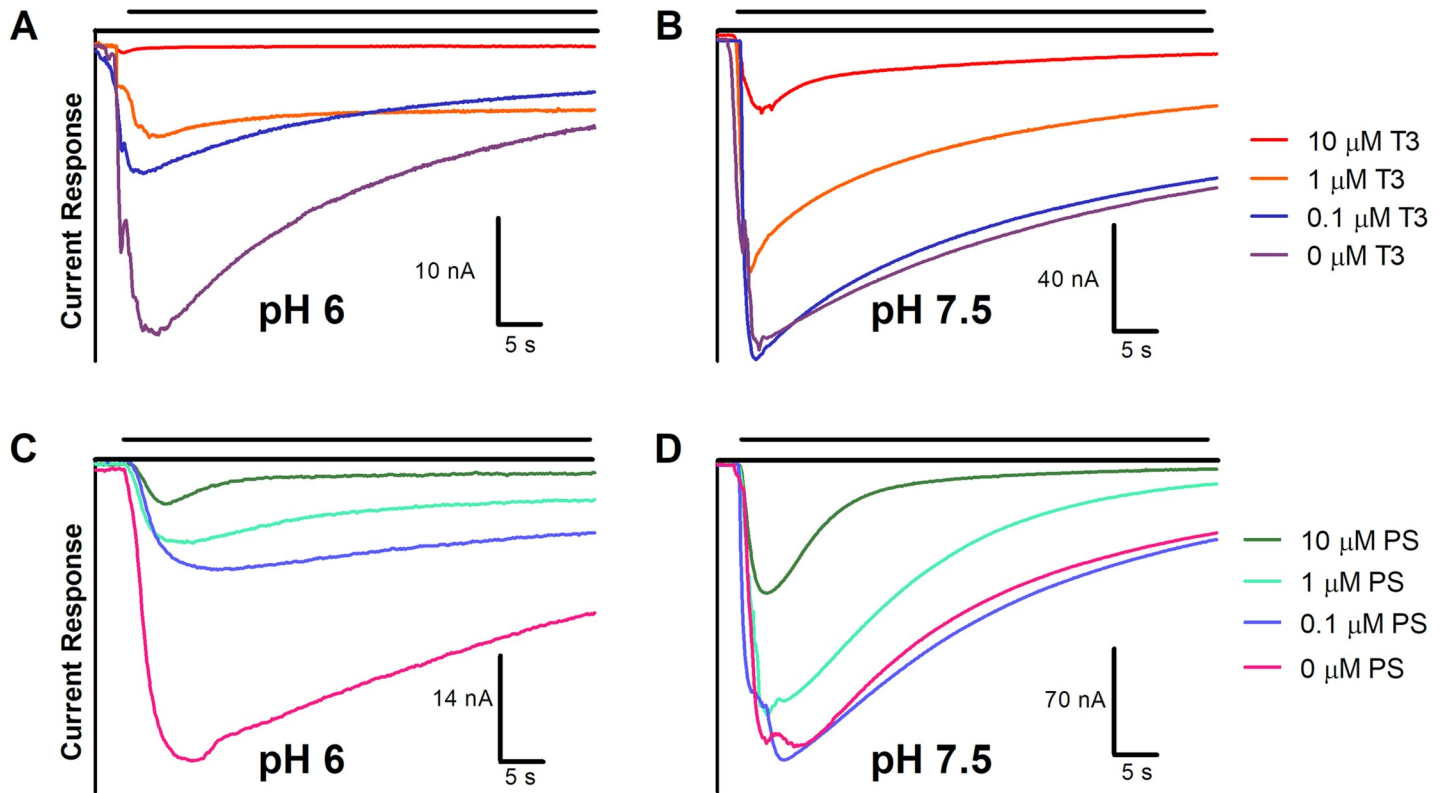
Fig 8. Effect of pH and T3 or PS on nAChR ion conductance. Raw current response traces after administration of 30 μM acetylcholine with the indicated dose of T3 or PS at pH 6 (A, C) or pH 7.5 (B, D). The single, representative traces are close to average values of curve-fit amplitude and decay rate (n = 2–3).

the decay rate of ion conductance. According to a two-way ANOVA, dose of inhibitor affects decay rate for both T3 ($P<0.0001$) and PS ($P<0.0001$; n = 3, per dose, per inhibitor) (Table 2, Table 3). The representative traces of a 10 μM dose of T3 or PS at each pH (6–9, in 0.5 pH increments) (Fig 9) demonstrate the effect due to ligand dose and pH on desensitization of the channel. According to a two-way ANOVA, at corresponding pHs, PS-inhibited channels exhibit a significantly different decay rate of ion conductance from T3 ($P<0.0001$) (Table 2). The effect of each ligand on nAChR desensitization may be involved with a region
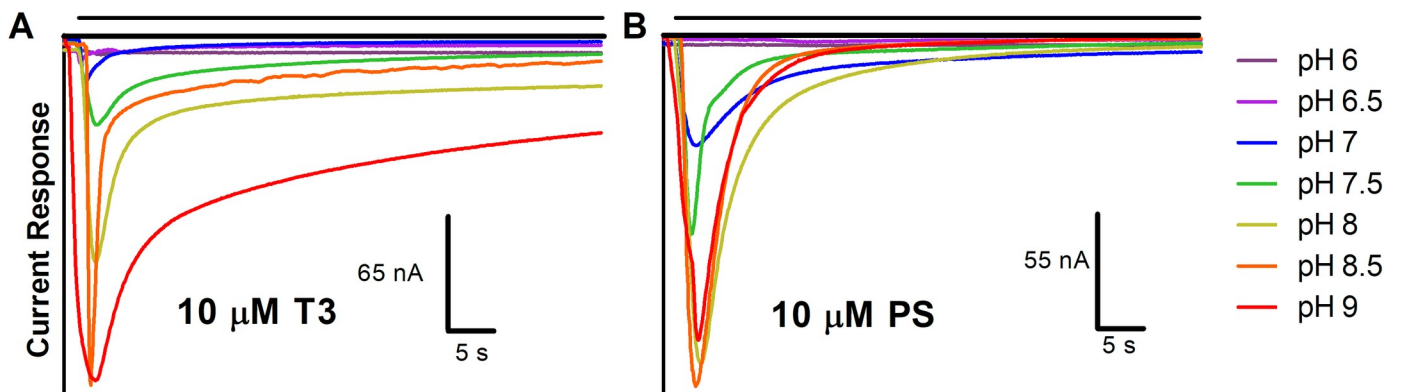
Fig 9. Effect of pH and 10 μM inhibitor on nAChR ion conductance. Raw current response traces after administration of 30 μM acetylcholine with (A) 10 μM T3 or (B) 10 μM PS at differing pH levels. The single, representative traces are close to average values of curve-fit amplitude and decay rate (n = 2–3).

Table 2. Decay Response for T3 and PS.

T3 Decay Response

	T3 Dose (μM)											
	0			0.1			1			10		
pH	Mean	SEM	N	Mean	SEM	N	Mean	SEM	N	Mean	SEM	N
6	17.7	2.5	2	23.1	2.3	2	10.0	3.2	3	0.4	0.2	2
6.5	26.4	4.2	3	28.0	4.9	3	7.8	0.4	3	1. 2	0.6	2
7	10.8	3.6	3	13.1	1.4	3	9.0	1.4	3	4.2	2.6	3
7.5	22.8	3.0	3	10.2	1.5	3	6.0	0.2	3	2.4	0.5	3
8	23.4	9.5	3	18.8	4.8	3	5.0	1. 2	3	3.6	1.7	3
8.5	12.1	1.0	3	11.7	1.2	3	2.9	0.6	3	1.0	0.3	2
9	5.2	4.1	3	14.8	2.0	3	14.0	7.2	3	13.6	11.0	3

PS Decay Response

	PS Dose (μM)											
	0			0.1			1			10		
pH	Mean	SEM	N	Mean	SEM	N	Mean	SEM	N	Mean	SEM	N
6	24.3	12.2	3	17.0	10.4	3	8.1	3.8	3	10.5	6.4	3
6.5	30.0	2.6	3	26.2	13.7	3	24.9	15.0	3	11.00	2.8	3
7	28.6	4.2	3	32.7	0.2	3	13.0	6.4	3	4.6	0.3	3
7.5	18.0	9.4	3	32.3	2.2	3	11.9	6.0	3	4.8	1.6	3
8	19.8	3.6	3	20.8	8.8	3	9.4	5.1	3	3.0	0.04	3
8.5	34.0	22.1	3	7.9	7.3	3	1.2	0.6	3	3.2	0.2	3
9	36.8	4.7	3	31.9	1.8	3	18.5	1.5	3	6. 4	1.6	3

https://doi.org/10.1371/journal.pone.0223272.t002

homologous to the desensitization gate structure of $GABA_A$ receptors, where PS has been shown to bind [38, 39]. This binding is theorized to cause constriction at the base of the channel pore, inducing a desensitized state [38]. Differences in binding site, orientation or binding affinity may cause differential effects on desensitization.

Discussion

Here we present the first direct observation of T3's inhibitory effect on nAChRs (Figs 2 and 6). The effect due to T3 on nAChRs is quantitatively similar to the effect due to T3 on $GABA_A$

Table 3. Statistical data for tests of T3 and PS inhibition[a].

	Factor	Deg of Freedom	F-value	P-value
2-way ANOVA: T3 inhibition decay rate vs. PS inhibition decay rate	Interaction	3	0.9816	0.4031
	Inhibitor	1	16.83	P<0.0001
	Dose	3	25.13	P<0.0001
	Residual	155		
2-way ANOVA: Doses of inhibitor (T3)	Interaction	18	2.068	0.0219
	Inhibitor	3	17.51	P<0.0001
	Dose	6	1.845	0.1088
	Residual	51		
2-way ANOVA: Doses of inhibitor (PS)	Interaction	18	0.6866	0.8094
	Inhibitor	3	11.82	P<0.0001
	Dose	6	1.497	0.1962
	Residual	56		

[a] 2-way ANOVAs were run for each parameter.

https://doi.org/10.1371/journal.pone.0223272.t003

receptors. For the first time, we also demonstrate an inhibitory effect due to PS on nAChR activity (Fig 2B). This effect is comparable to the inhibitory effect due to PS on $GABA_A$ receptors [57], and to T3's effect on nAChRs (Fig 2A) and $GABA_A$ receptors [29]. It has been hypothesized that lipophilic ligands have opposing functional effects on $GABA_A$ receptors and nAChRs, [45] but here we see this trend does not extend to PS and thyroid hormones.

T3 may act as a neurosteroid-like inhibitor of nAChRs. Thyroid hormone can access the brain via the blood-brain barrier [58–60]; nerve terminal fractions show T3 concentrations of 13.0–65 nM [61, 62], and synaptosomal T3 content is elevated 9.5 times in hypothyroid rats compared when compared to euthyroid rats [63]. Clinical presentations are associated with longer and less restful sleep in hypothyroid patients [64–66], and with insomnia and anxiety in hyperthyroid patients [67, 68]. When injected into the median preoptic nucleus of freely-moving adult rats, T3 increases REM sleep and wakefulness [69, 70], demonstrating short-term, nongenomic effects on behavior. T3 also directly inhibits $GABA_A$ receptor activity *in vitro* [29, 34]. The similarity of effects due to T3 and due to neurosteroids, which also modulate sleep [71–74] and anxiety [75, 76], may indicate similar mode of action due to T3 and neurosteroids.

Further, T3 structure resembles the structure of neurosteroids. While it lacks a steroid's fundamental four-ring molecular group, T3 has a nearly identical volume and shape to PS [33]. Based on molecular dynamics simulations in which the two molecules favorably occupy TM-localized regions, in conjunction with $GABA_A$R binding data, Westergard et al. posit that T3 and the PS-like molecule allopregnanolone have a shared binding site in $GABA_A$ receptors [29]. This would indicate a possible similar mode of T3 action to that of neurosteroids.

T3 appears to be an exception to established neurosteroid structure-activity relationships. Here we may reject the hypothesis that a population of anionic T3 transduces the inhibitory effect of T3 in nAChR. Further study using analogues of T3 with singular changes in functional groups (e.g., the presence or absence of an amino group, or of bulky and non-bulky groups) may be required to isolate the molecular origin of its unexpected inhibitory effects.

We show here that T3 and PS both affect channel desensitization. Further, changing environmental pH levels appear to affect T3 and PS-induced nAChR desensitization. This may be a result of pH influence on channel residues at the TMD, as has been suggested by previous investigations [54, 55].

The present work adds to the mounting evidence of T3's nongenomic effect on adult brain tissue [34, 69, 70, 77–80]. These effects may be mediated through interactions with the nAChRs, with $GABA_A$ receptors, or with both. This work also indicates, through the inhibitory action of PS and the inhibitory, neurosteroid-like action of T3 on the nAChR, a complex structure-function relationship. The actions of both ligands relative to one another, and to the nearly identical molecules allopregnanolone and triac, can be a tool to investigate binding and inhibition of the channel.

Author Contributions

Conceptualization: Steven X. Moffett, Grace Brannigan, Joseph V. Martin.

Data curation: Steven X. Moffett, Grace Brannigan, Joseph V. Martin.

Formal analysis: Steven X. Moffett, Eric A. Klein, Grace Brannigan, Joseph V. Martin.

Funding acquisition: Grace Brannigan, Joseph V. Martin.

Investigation: Steven X. Moffett.

Methodology: Steven X. Moffett, Eric A. Klein, Grace Brannigan, Joseph V. Martin.

Project administration: Grace Brannigan, Joseph V. Martin.

Resources: Grace Brannigan, Joseph V. Martin.

Software: Grace Brannigan, Joseph V. Martin.

Supervision: Grace Brannigan, Joseph V. Martin.

Visualization: Steven X. Moffett, Joseph V. Martin.

Writing – original draft: Steven X. Moffett.

Writing – review & editing: Steven X. Moffett, Eric A. Klein, Grace Brannigan, Joseph V. Martin.

References

1. Clarke PB, Schwartz RD, Paul SM, Pert CB, Pert A. Nicotinic binding in rat brain: autoradiographic comparison of [3H]acetylcholine, [3H]nicotine, and [125I]-alpha-bungarotoxin. The Journal of neuroscience: the official journal of the Society for Neuroscience. 1985; 5(5):1307–15. Epub 1985/05/01. PMID: 3998824.

2. Hucho F. The nicotinic acetylcholine receptor and its ion channel. European journal of biochemistry. 1986; 158(2):211–26. Epub 1986/07/15. https://doi.org/10.1111/j.1432-1033.1986.tb09740.x PMID: 2426106.

3. Steinlein OK, Bertrand D. Nicotinic receptor channelopathies and epilepsy. Pflugers Archiv: European journal of physiology. 2010; 460(2):495–503. Epub 2009/12/18. https://doi.org/10.1007/s00424-009-0766-8 PMID: 20016990.

4. Fambrough DM, Drachman DB, Satyamurti S. Neuromuscular junction in myasthenia gravis: decreased acetylcholine receptors. Science (New York, NY). 1973; 182(4109):293–5. Epub 1973/10/19. https://doi.org/10.1126/science.182.4109.293 PMID: 4742736.

5. Drachman DB, Angus CW, Adams RN, Michelson JD, Hoffman GJ. Myasthenic antibodies cross-link acetylcholine receptors to accelerate degradation. The New England journal of medicine. 1978; 298 (20):1116–22. Epub 1978/05/18. https://doi.org/10.1056/NEJM197805182982004 PMID: 643030.

6. Sine SM, Engel AG. Recent advances in Cys-loop receptor structure and function. Nature. 2006; 440 (7083):448–55. Epub 2006/03/24. https://doi.org/10.1038/nature04708 PMID: 16554804.

7. Lester HA, Dibas MI, Dahan DS, Leite JF, Dougherty DA. Cys-loop receptors: new twists and turns. Trends in neurosciences. 2004; 27(6):329–36. Epub 2004/05/29. https://doi.org/10.1016/j.tins.2004.04.002 PMID: 15165737.

8. Thompson AJ, Lester HA, Lummis SC. The structural basis of function in Cys-loop receptors. Quarterly reviews of biophysics. 2010; 43(4):449–99. Epub 2010/09/21. https://doi.org/10.1017/S0033583510000168 PMID: 20849671.

9. Miller PS, Smart TG. Binding, activation and modulation of Cys-loop receptors. Trends in pharmacological sciences. 2010; 31(4):161–74. Epub 2010/01/26. https://doi.org/10.1016/j.tips.2009.12.005 PMID: 20096941.

10. Lynagh T, Laube B. Opposing effects of the anesthetic propofol at pentameric ligand-gated ion channels mediated by a common site. The Journal of neuroscience: the official journal of the Society for Neuroscience. 2014; 34(6):2155–9. Epub 2014/02/07. https://doi.org/10.1523/jneurosci.4307-13.2014 PMID: 24501356.

11. Miyazawa A, Fujiyoshi Y, Unwin N. Structure and gating mechanism of the acetylcholine receptor pore. Nature. 2003; 423(6943):949–55. Epub 2003/06/27. https://doi.org/10.1038/nature01748 PMID: 12827192.

12. Corringer PJ, Poitevin F, Prevost MS, Sauguet L, Delarue M, Changeux JP. Structure and pharmacology of pentameric receptor channels: from bacteria to brain. Structure (London, England: 1993). 2012; 20(6):941–56. Epub 2012/06/12. https://doi.org/10.1016/j.str.2012.05.003 PMID: 22681900.

13. Atluri N, Joksimovic SM, Oklopcic A, Milanovic D, Klawitter J, Eggan P, et al. A neurosteroid analogue with T-type calcium channel blocking properties is an effective hypnotic, but is not harmful to neonatal rat brain. British journal of anaesthesia. 2018; 120(4):768–78. Epub 2018/03/27. https://doi.org/10.1016/j.bja.2017.12.039 PMID: 29576117; PubMed Central PMCID: PMC6200096.

14. Zhang M, Liu J, Zhou MM, Wu H, Hou Y, Li YF, et al. Anxiolytic effects of hippocampal neurosteroids in normal and neuropathic rats with spared nerve injury. Journal of neurochemistry. 2017; 141(1):137–50. Epub 2017/01/28. https://doi.org/10.1111/jnc.13965 PMID: 28129443.

15. Gulinello M, Smith SS. Anxiogenic effects of neurosteroid exposure: sex differences and altered GABAA receptor pharmacology in adult rats. The Journal of pharmacology and experimental therapeutics. 2003; 305(2):541–8. Epub 2003/02/28. https://doi.org/10.1124/jpet.102.045120 PMID: 12606703.

16. Frye CA. The neurosteroid 3 alpha, 5 apha-THP has antiseizure and possible neuroprotective effects in an animal model of epilepsy. Brain research. 1995; 696(1–2):113–20. Epub 1995/10/23. https://doi.org/10.1016/0006-8993(95)00793-p PMID: 8574658.

17. Joksimovic SL, Covey DF, Jevtovic-Todorovic V, Todorovic SM. Neurosteroids in Pain Management: A New Perspective on an Old Player. Frontiers in pharmacology. 2018; 9:1127. Epub 2018/10/20. https://doi.org/10.3389/fphar.2018.01127 PMID: 30333753; PubMed Central PMCID: PMC6176051.

18. Belelli D, Pistis M, Peters JA, Lambert JJ. The interaction of general anaesthetics and neurosteroids with GABA(A) and glycine receptors. Neurochemistry international. 1999; 34(5):447–52. Epub 1999/07/09. https://doi.org/10.1016/s0197-0186(99)00037-6 PMID: 10397373.

19. Li GD, Chiara DC, Cohen JB, Olsen RW. Neurosteroids allosterically modulate binding of the anesthetic etomidate to gamma-aminobutyric acid type A receptors. The Journal of biological chemistry. 2009; 284 (18):11771–5. Epub 2009/03/14. https://doi.org/10.1074/jbc.C900016200 PMID: 19282280; PubMed Central PMCID: PMC2673245.

20. Covey DF, Evers AS, Mennerick S, Zorumski CF, Purdy RH. Recent developments in structure-activity relationships for steroid modulators of GABA(A) receptors. Brain research Brain research reviews. 2001; 37(1–3):91–7. Epub 2001/12/18. PMID: 11744077.

21. Covey DF, Han M, Kumar AS, de La Cruz MA, Meadows ES, Hu Y, et al. Neurosteroid analogues. 8. Structure-activity studies of N-acylated 17a-aza-D-homosteroid analogues of the anesthetic steroids (3alpha, 5alpha)- and (3alpha,5beta)-3-hydroxypregnan-20-one. Journal of medicinal chemistry. 2000; 43(17):3201–4. Epub 2000/09/01. https://doi.org/10.1021/jm0002477 PMID: 10966737.

22. Covey DF, Nathan D, Kalkbrenner M, Nilsson KR, Hu Y, Zorumski CF, et al. Enantioselectivity of pregnanolone-induced gamma-aminobutyric acid(A) receptor modulation and anesthesia. The Journal of pharmacology and experimental therapeutics. 2000; 293(3):1009–16. Epub 2000/06/28. PMID: 10869405.

23. Paradiso K, Sabey K, Evers AS, Zorumski CF, Covey DF, Steinbach JH. Steroid inhibition of rat neuronal nicotinic alpha4beta2 receptors expressed in HEK 293 cells. Molecular pharmacology. 2000; 58 (2):341–51. Epub 2000/07/25. https://doi.org/10.1124/mol.58.2.341 PMID: 10908302.

24. Uki M, Nabekura J, Akaike N. Suppression of the nicotinic acetylcholine response in rat superior cervical ganglionic neurons by steroids. Journal of neurochemistry. 1999; 72(2):808–14. Epub 1999/02/04. https://doi.org/10.1046/j.1471-4159.1999.0720808.x PMID: 9930757.

25. Wang M. Neurosteroids and GABA-A Receptor Function. Frontiers in endocrinology. 2011; 2:44. Epub 2011/01/01. https://doi.org/10.3389/fendo.2011.00044 PMID: 22654809; PubMed Central PMCID: PMC3356040.

26. Belelli D, Casula A, Ling A, Lambert JJ. The influence of subunit composition on the interaction of neurosteroids with GABA(A) receptors. Neuropharmacology. 2002; 43(4):651–61. Epub 2002/10/09. https://doi.org/10.1016/s0028-3908(02)00172-7 PMID: 12367610.

27. Hosie AM, Clarke L, da Silva H, Smart TG. Conserved site for neurosteroid modulation of https://doi.org/10.1016/j.neuropharm.2008.07.050 PMID: 18762201 A receptors. Neuropharmacology. 2009; 56 (1):149–54. Epub 2008/09/03.

28. Seljeset S, Bright DP, Thomas P, Smart TG. Probing GABAA receptors with inhibitory neurosteroids. Neuropharmacology. 2018; 136(Pt A):23–36. Epub 2018/02/16. https://doi.org/10.1016/j.neuropharm.2018.02.008 PMID: 29447845; PubMed Central PMCID: PMC6018617.

29. Westergard T, Salari R, Martin JV, Brannigan G. Interactions of L-3,5,3'-Triiodothyronine [corrected], Allopregnanolone, and Ivermectin with the GABAA Receptor: Evidence for Overlapping Intersubunit Binding Modes. PLoS one. 2015; 10(9):e0139072. Epub 2015/10/01. https://doi.org/10.1371/journal.pone.0139072 PMID: 26421724; PubMed Central PMCID: PMC4589331.

30. Majewska MD. Neurosteroids: endogenous bimodal modulators of the GABAA receptor. Mechanism of action and physiological significance. Progress in neurobiology. 1992; 38(4):379–95. Epub 1992/01/01. PMID: 1349441.

31. Majewska MD, Harrison NL, Schwartz RD, Barker JL, Paul SM. Steroid hormone metabolites are barbiturate-like modulators of the GABA receptor. Science (New York, NY). 1986; 232(4753):1004–7. Epub 1986/05/23. https://doi.org/10.1126/science.2422758 PMID: 2422758.

32. Callachan H, Cottrell GA, Hather NY, Lambert JJ, Nooney JM, Peters JA. Modulation of the GABAA receptor by progesterone metabolites. Proceedings of the Royal Society of London Series B, Biological sciences. 1987; 231(1264):359–69. Epub 1987/08/21. https://doi.org/10.1098/rspb.1987.0049 PMID: 2888123.

33. Martin JV, Padron JM, Newman MA, Chapell R, Leidenheimer NJ, Burke LA. Inhibition of the activity of the native gamma-aminobutyric acid A receptor by metabolites of thyroid hormones: correlations with molecular modeling studies. Brain research. 2004; 1004(1–2):98–107. Epub 2004/03/23. https://doi.org/10.1016/j.brainres.2003.12.043 PMID: 15033424.

34. Martin JV, Williams DB, Fitzgerald RM, Im HK, Vonvoigtlander PF. Thyroid hormonal modulation of the binding and activity of the GABAA receptor complex of brain. Neuroscience. 1996; 73(3):705–13. Epub 1996/08/01. https://doi.org/10.1016/0306-4522(96)00052-8 PMID: 8809792.

35. Chapell R, Martin J, Machu TK, Leidenheimer NJ. Direct channel-gating and modulatory effects of triiodothyronine on recombinant GABA(A) receptors. European journal of pharmacology. 1998; 349 (1):115–21. Epub 1998/07/21. https://doi.org/10.1016/s0014-2999(98)00182-4 PMID: 9669504.

36. Puia G, Losi G. Thyroid hormones modulate GABA(A) receptor-mediated currents in hippocampal neurons. Neuropharmacology. 2011; 60(7–8):1254–61. Epub 2011/01/11. https://doi.org/10.1016/j.neuropharm.2010.12.013 PMID: 21215272.

37. Majewska MD, Mienville JM, Vicini S. Neurosteroid pregnenolone sulfate antagonizes electrophysiological responses to GABA in neurons. Neuroscience letters. 1988; 90(3):279–84. Epub 1988/08/01. https://doi.org/10.1016/0304-3940(88)90202-9 PMID: 3138576.

38. Laverty D, Thomas P, Field M, Andersen OJ, Gold MG, Biggin PC, et al. Crystal structures of a GABAA-receptor chimera reveal new endogenous neurosteroid-binding sites. Nature structural & molecular biology. 2017; 24(11):977–85. Epub 2017/10/03. https://doi.org/10.1038/nsmb.3477 PMID: 28967882.

39. Gielen M, Thomas P, Smart TG. The desensitization gate of inhibitory Cys-loop receptors. Nature communications. 2015; 6:6829. Epub 2015/04/22. https://doi.org/10.1038/ncomms7829 PMID: 25891813; PubMed Central PMCID: PMC4410641.

40. Corrie J, Ogrel AA, McCardy EA, Blanton MP, Baenziger JE. Lipid-protein interactions at the nicotinic acetylcholine receptor A functional coupling between nicotinic receptors and phosphatidic acid-containing lipid bilayers. Journal of Biological Chemistry. 2002; 277(1):201–8. https://doi.org/10.1074/jbc.M108341200 PMID: 11682482

41. daCosta CJ, Ogrel AA, McCardy EA, Blanton MP, Baenziger JE. Lipid-protein interactions at the nicotinic acetylcholine receptor. A functional coupling between nicotinic receptors and phosphatidic acid-containing lipid bilayers. The Journal of biological chemistry. 2002; 277(1):201–8. Epub 2001/10/30. https://doi.org/10.1074/jbc.M108341200 PMID: 11682482.

42. Sharp L, Salari R, Brannigan G. Boundary lipids of the nicotinic acetylcholine receptor: spontaneous partitioning via coarse-grained molecular dynamics simulation. Biochimica et Biophysica Acta (BBA)-Biomembranes. 2019.

43. Rankin SE, Addona GH, Kloczewiak MA, Bugge B, Miller KW. The cholesterol dependence of activation and fast desensitization of the nicotinic acetylcholine receptor. Biophysical journal. 1997; 73(5):2446–55. Epub 1997/11/25. https://doi.org/10.1016/S0006-3495(97)78273-0 PMID: 9370438; PubMed Central PMCID: PMC1181146.

44. Criado M, Eibl H, Barrantes FJ. Effects of lipids on acetylcholine receptor. Essential need of cholesterol for maintenance of agonist-induced state transitions in lipid vesicles. Biochemistry. 1982; 21(15):3622–9. Epub 1982/07/20. https://doi.org/10.1021/bi00258a015 PMID: 7115688.

45. Campagna JA, Miller KW, Forman SA. Mechanisms of actions of inhaled anesthetics. The New England journal of medicine. 2003; 348(21):2110–24. Epub 2003/05/23. https://doi.org/10.1056/NEJMra021261 PMID: 12761368.

46. Ke L, Lukas RJ. Effects of steroid exposure on ligand binding and functional activities of diverse nicotinic acetylcholine receptor subtypes. Journal of neurochemistry. 1996; 67(3):1100–12. Epub 1996/09/01. https://doi.org/10.1046/j.1471-4159.1996.67031100.x PMID: 8752117.

47. Barrantes FJ, Antollini SS, Bouzat CB, Garbus I, Massol RH. Nongenomic effects of steroids on the nicotinic acetylcholine receptor. Kidney international. 2000; 57(4):1382–9. Epub 2000/04/12. https://doi.org/10.1046/j.1523-1755.2000.00979.x PMID: 10760071.

48. Blanton MP, Xie Y, Dangott LJ, Cohen JB. The steroid promegestone is a noncompetitive antagonist of the Torpedo nicotinic acetylcholine receptor that interacts with the lipid-protein interface. Molecular pharmacology. 1999; 55(2):269–78. Epub 1999/02/03. https://doi.org/10.1124/mol.55.2.269 PMID: 9927618.

49. Hamouda AK, Stewart DS, Husain SS, Cohen JB. Multiple transmembrane binding sites for p-trifluoromethyldiazirinyl-etomidate, a photoreactive Torpedo nicotinic acetylcholine receptor allosteric inhibitor. The Journal of biological chemistry. 2011; 286(23):20466–77. Epub 2011/04/19. https://doi.org/10.1074/jbc.M111.219071 PMID: 21498509; PubMed Central PMCID: PMC3121496.

50. McGrath M, Yu Z, Jayakar SS, Ma C, Tolia M, Zhou X, et al. Etomidate and Etomidate Analog Binding and Positive Modulation of gamma-Aminobutyric Acid Type A Receptors: Evidence for a State-

dependent Cutoff Effect. Anesthesiology. 2018; 129(5):959–69. Epub 2018/07/28. https://doi.org/10.1097/ALN.0000000000002356 PMID: 30052529; PubMed Central PMCID: PMC6278829.

51. Sooksawate T, Simmonds MA. Effects of membrane cholesterol on the sensitivity of the GABA(A) receptor to GABA in acutely dissociated rat hippocampal neurones. Neuropharmacology. 2001; 40 (2):178–84. Epub 2000/12/15. https://doi.org/10.1016/s0028-3908(00)00159-3 PMID: 11114396.

52. Baenziger JE, Domville JA, Therien JPD. The Role of Cholesterol in the Activation of Nicotinic Acetylcholine Receptors. Current topics in membranes. 2017; 80:95–137. Epub 2017/09/03. https://doi.org/10.1016/bs.ctm.2017.05.002 PMID: 28863823.

53. Kudo K, Tachikawa E, Kashimoto T. Inhibition by pregnenolone sulfate of nicotinic acetylcholine response in adrenal chromaffin cells. European journal of pharmacology. 2002; 456(1–3):19–27. https://doi.org/10.1016/s0014-2999(02)02623-7 PMID: 12450565

54. Palma A, Li L, Chen XJ, Pappone P, McNamee M. Effects of pH on acetylcholine receptor function. The Journal of membrane biology. 1991; 120(1):67–73. Epub 1991/02/01. https://doi.org/10.1007/bf01868592 PMID: 2020020.

55. li L, McNamee M. Modulation of Nicotinic Acetylcholine Receptor Channel by pH: A Difference in pH Sensitivity of Torpedo and Mouse Receptors Expressed in Xenopus Oocytes. Cellular and Molecular Biology. 1991; 12(2):83–93.

56. Ochoa EL, Dalziel AW, McNamee MG. Reconstitution of acetylcholine receptor function in lipid vesicles of defined composition. Biochimica et biophysica acta. 1983; 727(1):151–62. Epub 1983/01/05. https://doi.org/10.1016/0005-2736(83)90379-6 PMID: 6824649.

57. Mienville JM, Vicini S. Pregnenolone sulfate antagonizes GABAA receptor-mediated currents via a reduction of channel opening frequency. Brain research. 1989; 489(1):190–4. Epub 1989/06/05. https://doi.org/10.1016/0006-8993(89)90024-3 PMID: 2472854.

58. Dratman MB, Futaesaku Y, Crutchfield FL, Berman N, Payne B, Sar M, et al. Iodine-125-labeled triiodothyronine in rat brain: evidence for localization in discrete neural systems. Science (New York, NY). 1982; 215(4530):309–12. Epub 1982/01/15. https://doi.org/10.1126/science.7053582 PMID: 7053582.

59. Dratman MB, Crutchfield FL, Axelrod J, Colburn RW, Thoa N. Localization of triiodothyronine in nerve ending fractions of rat brain. Proceedings of the National Academy of Sciences of the United States of America. 1976; 73(3):941–4. Epub 1976/03/01. https://doi.org/10.1073/pnas.73.3.941 PMID: 1062808; PubMed Central PMCID: PMC336036.

60. Dratman MB, Crutchfield FL. Synaptosomal [125I]triiodothyronine after intravenous [125I]thyroxine. The American journal of physiology. 1978; 235(6):E638–47. Epub 1978/12/01. https://doi.org/10.1152/ajpendo.1978.235.6.E638 PMID: 736123.

61. Mason GA, Walker CH, Prange AJ Jr. L-triiodothyronine: is this peripheral hormone a central neurotransmitter? Neuropsychopharmacology: official publication of the American College of Neuropsychopharmacology. 1993; 8(3):253–8. Epub 1993/05/01. https://doi.org/10.1038/npp.1993.28 PMID: 8099484.

62. Sarkar PK, Ray AK. Specific binding of L-triiodothyronine modulates Na(+)-K(+)-ATPase activity in adult rat cerebrocortical synaptosomes. Neuroreport. 1998; 9(6):1149–52. Epub 1998/05/28. https://doi.org/10.1097/00001756-199804200-00035 PMID: 9601684.

63. Sarkar PK, Ray AK. Synaptosomal T3 content in cerebral cortex of adult rat in different thyroidal states. Neuropsychopharmacology: official publication of the American College of Neuropsychopharmacology. 1994; 11(3):151–5. Epub 1994/11/01. https://doi.org/10.1038/sj.npp.1380101 PMID: 7865096.

64. Gunnarsson T, Sjöberg S, Eriksson M, Nordin C. Depressive symptoms in hypothyroid disorder with some observations on biochemical correlates. Neuropsychobiology. 2001; 43(2):70–4. https://doi.org/10.1159/000054869 PMID: 11174048

65. Madhu K. Sleep in young untreated hypothyroid subjects. J Sleep Res. 1996; 5(3):198–9. PMID: 8956211

66. Whybrow Bauer. Behavioral and psychiatric aspects of hypothyroidism. Braverman LE UR, editor. Philadelphia: Lippincott Williams and Wilkins; 2005.

67. Demet MM, Ozmen B, Deveci A, Boyvada S, Adiguzel H, Aydemir O. Depression and anxiety in hyperthyroidism. Archives of medical research. 2002; 33(6):552–6. Epub 2002/12/31. PMID: 12505101.

68. Whybrow Bauer. Behavioral and psychiatric aspects of thyrotoxicosis. Braverman LE UR, editor. Philadelphia: Lippincott Williams and Wilkins; 2005.

69. Martin JV, Giannopoulos PF, Moffett SX, James TD. Effects of acute microinjections of thyroid hormone to the preoptic region of euthyroid adult male rats on sleep and motor activity. Brain research. 2013; 1516:45–54. Epub 2013/01/26. https://doi.org/10.1016/j.brainres.2013.01.032 PMID: 23348377.

70. Moffett SX, Giannopoulos PF, James TD, Martin JV. Effects of acute microinjections of thyroid hormone to the preoptic region of hypothyroid adult male rats on sleep, motor activity and body temperature.

Brain research. 2013; 1516:55–65. Epub 2013/04/23. https://doi.org/10.1016/j.brainres.2013.04.017 PMID: 23603414.

71. Steiger A, Trachsel L, Guldner J, Hemmeter U, Rothe B, Rupprecht R, et al. Neurosteroid pregnenolone induces sleep-EEG changes in man compatible with inverse agonistic GABAA-receptor modulation. Brain research. 1993; 615(2):267–74. https://doi.org/10.1016/0006-8993(93)90037-n PMID: 8395958

72. Darnaudery M, Pallares M, Bouyer J, Le Moal M, Mayo W. Infusion of neurosteroids into the rat nucleus basalis affects paradoxical sleep in accordance with their memory modulating properties. Neuroscience. 1999; 92(2):583–8. https://doi.org/10.1016/s0306-4522(99)00019-6 PMID: 10408607

73. Lancel M, Faulhaber J, Holsboer F, Rupprecht R. Progesterone induces changes in sleep comparable to those of agonistic GABAA receptor modulators. American Journal of Physiology-Endocrinology and Metabolism. 1996; 271(4):E763–E72.

74. Damianisch K, Rupprecht R, Lancel M. The influence of subchronic administration of the neurosteroid allopregnanolone on sleep in the rat. Neuropsychopharmacology: official publication of the American College of Neuropsychopharmacology. 2001; 25(4):576–84.

75. Shen H, Gong QH, Aoki C, Yuan M, Ruderman Y, Dattilo M, et al. Reversal of neurosteroid effects at α4β2δ GABA A receptors triggers anxiety at puberty. Nature neuroscience. 2007; 10(4):469. https://doi.org/10.1038/nn1868 PMID: 17351635

76. Longone P, Rupprecht R, Manieri GA, Bernardi G, Romeo E, Pasini A. The complex roles of neurosteroids in depression and anxiety disorders. Neurochemistry international. 2008; 52(4–5):596–601. https://doi.org/10.1016/j.neuint.2007.10.001 PMID: 17996986

77. Sarkar PK, Durga ND, Morris JJ, Martin JV. In vitro thyroid hormone rapidly modulates protein phosphorylation in cerebrocortical synaptosomes from adult rat brain. Neuroscience. 2006; 137(1):125–32. Epub 2005/11/18. https://doi.org/10.1016/j.neuroscience.2005.10.002 PMID: 16289831.

78. Sarkar PK, Morris JJ, Martin JV. Non-genomic effect of L-triiodothyronine on calmodulin-dependent synaptosomal protein phosphorylation in adult rat cerebral cortex. Indian journal of experimental biology. 2011; 49(3):169–76. Epub 2011/04/02. PMID: 21452595.

79. James TD, Moffett SX, Scanlan TS, Martin JV. Effects of acute microinjections of the thyroid hormone derivative 3-iodothyronamine to the preoptic region of adult male rats on sleep, thermoregulation and motor activity. Hormones and behavior. 2013; 64(1):81–8. https://doi.org/10.1016/j.yhbeh.2013.05.004 PMC4091812. PMID: 23702093

80. Dratman MB, Gordon JT. Thyroid hormones as neurotransmitters. Thyroid: official journal of the American Thyroid Association. 1996; 6(6):639–47. Epub 1996/12/01. https://doi.org/10.1089/thy.1996.6.639 PMID: 9001201.